Reprinted from December 1986, Vol. 108, Journal of Applied Mechanics

Large Deflection Stability of Spherical Shells With Ring Loads

J. Cagan[1]
Assoc. Mem. ASME

L. A. Taber
Assoc. Mem. ASME

Department of Mechanical Engineering,
University of Rochester,
Rochester, NY 14627

Large deflections of shallow and deep spherical shells under ring loads are studied. The axisymmetric problem is solved through a Newton-Raphson technique on discretized nonlinear shell equations. Comparison of computed load-deflection curves to experimental data from both thick and thin shells generally shows good agreement in peak loads and the type of instability. For a point load, the load increases monotonically with deflection; as the ring radius increases, transition-type (snap-through) and then local buckling occurs. In addition, the pre- and post-buckled mechanical behaviors of the shell are examined.

Introduction

Previous work pertaining to the deformation of spherical shells under ring loads has been rather limited. Experimental work was done by Evan-Iwanowski et al. (1963), who investigated buckling of thin, shallow, spherical shells with this type of loading. They found that if the ring diameter is less than some minimum value, the shell does not buckle. Otherwise, the shell either snap-buckles or, for large rings, buckles locally (Fig. 1). Snap-through, or transition buckling (Fig. 1*a*), implies that past a critical point of a load versus deflection curve, a smooth, continuous transition takes place from relatively stiff ring-type to a softer point-load-type behavior, as a dimple of reversed curvature forms gradually. On the other hand, with ring deflection specified, local buckling (Fig. 1*b*) exhibits a discontinuity at a critical point as the load jumps suddenly to a much smaller value, with the dimple forming abruptly. Since local buckling curves also include a deflection snap (for a specified load), we will refer to "snap-through" buckling as "transition" buckling herein.

Taber (1983) presented experimental results for the deflection of both fluid-filled and empty hemispherical rubber shells due to solid cylindrical indenters. As the deflection increases, the load-deflection curves for an empty shell initially resemble those due to a flat plate but eventually fall back toward the point-load curve as the indenter becomes immersed within a dimple of reversed curvature, with the indenter now applying essentially a ring load. The deformation can occur with or without a peak in load, depending on the indenter radius. As found by Evan-Iwanowski et al. (1963), there is a minimum radius below which no peak occurs; yet this is a different situation in that the indenter acts as a ring load only after it is immersed within the dimple.

Pieces of the ring load problem have been studied analytically. Using an energy method, Chien and Hu (1956) computed the critical load for "oil canning," or transition buckling, of a thin spherical cap due to a ring load. With an implicit numerical technique, which involved a Newton-Raphson scheme on integral matrices, Parnell (1984) solved Reissner's (1950) nonlinear shell equations for moderate rotation. Limited application to shallow spherical caps deformed by ring loads showed only transition-type buckling. In other work, Wan (1984) constructed asymptotic solutions to study the fundamental behavior for polar dimpling of spherical shells with ring and other similar loadings, while Updike and Kalnins (1970, 1972) examined the related problem of a spherical shell compressed between rigid plates.

In this paper, we will apply Parnell's (1984) method to steep and shallow, thin and thick, spherical shells. Both local and transition buckling will be studied, along with the mechanical

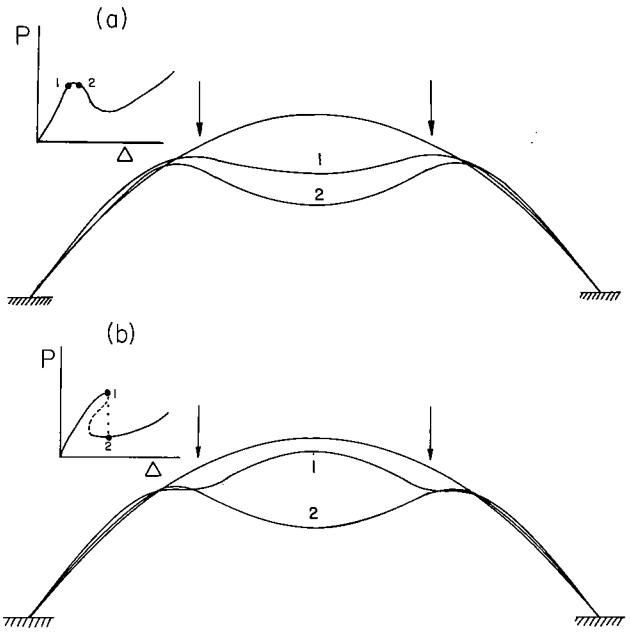

Fig. 1 Typical load-deflection curves and corresponding deflection shapes for ring load on spherical shell: (*a*) transition buckling; (*b*) local buckling

[1]Presently at the Eastman Kodak Company, Engineering Technology Laboratory, Rochester, NY 14650.

Contributed by the Applied Mechanics Division for publication in the JOURNAL OF APPLIED MECHANICS.

Discussion on this paper should be addressed to the Editorial Department, ASME, United Engineering Center, 345 East 47th Street, New York, N.Y. 10017, and will be accepted until two months after final publication of the paper itself in the JOURNAL OF APPLIED MECHANICS. Manuscript received by ASME Applied Mechanics Division, October 31, 1985; final revision April 24, 1986.

behavior of the shell around the critical points. Comparison with experimental data from Evan-Iwanowski et al. (1963) demonstrates the accuracy of the analytical solution. In addition, computed results are compared to new data from experiments on deep shells deflected by solid indenters.

Solution Technique

In state-vector form, the nonlinear equations of Reissner (1950) for moderate rotation of a thin shell of revolution are (Parnell, 1984)

$$\frac{d\mathbf{y}}{ds}=\mathbf{A}\cdot\mathbf{y}+\mathbf{N}(\mathbf{y}) \tag{1}$$

where the solution vector is

$$\mathbf{y}^T=[rM_\phi, rH, rV, \chi, h, v], \tag{2}$$

the linear terms are given by

$$\mathbf{A}=\begin{bmatrix} \nu\cos\phi & \sin\phi & -\cos\phi & \frac{Et^3}{12}\frac{\cos^2\phi}{r} & 0 & 0 \\ 0 & \frac{\nu}{r}\cos\phi & -\frac{\nu}{r}\sin\phi & 0 & \frac{Et}{r} & 0 \\ 0 & 0 & 0 & 0 & 0 & 0 \\ (rEtc^2)^{-1} & 0 & 0 & -\frac{\nu}{r}\cos\phi & 0 & 0 \\ 0 & \frac{1-\nu^2}{rEt}\cos^2\phi & \frac{1-\nu^2}{rEt}\sin\phi\cos\phi & -\sin\phi & -\frac{\nu}{r}\cos\phi & 0 \\ 0 & \frac{1-\nu^2}{rEt}\sin\phi\cos\phi & \frac{1-\nu^2}{rEt}\sin^2\phi & \cos\phi & -\frac{\nu}{r}\sin\phi & 0 \end{bmatrix}, \tag{3}$$

the nonlinear contribution is

$$\mathbf{N}(\mathbf{y})=\begin{bmatrix} \chi(rH\cos\phi+rV\sin\phi) \\ 0 \\ 0 \\ 0 \\ -\chi^2\cos\phi/2 \\ -\chi^2\sin\phi/2 \end{bmatrix}, \tag{4}$$

and surface load terms are deleted.

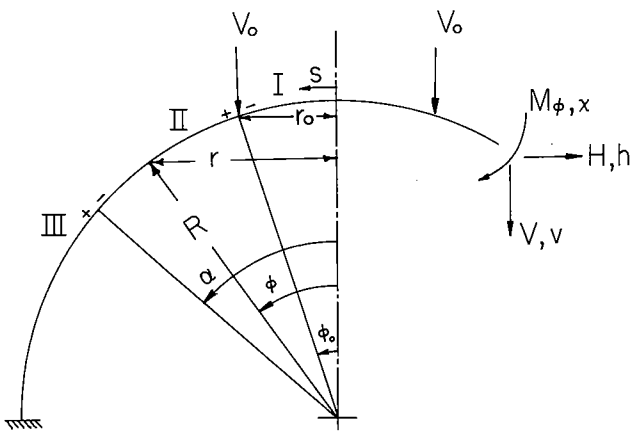

Fig. 2 Geometry and force system for spherical shell with ring load

In these equations M_ϕ, H, V, χ, h, v are the meridional bending moment, horizontal and vertical force resultants, rotation, and horizontal and vertical displacements, respectively (Fig. 2). Also, ν is Poisson's ratio, E is Young's modulus, and t is the shell thickness.

Consider now a vertical ring load of radius r_0 and magnitude $P = 2\pi r_0 V_0$ on a clamped spherical shell of radius R (Fig. 2). The appropriate regularity and boundary conditions are

$$rV=\chi=h=0 \quad \text{at} \quad \phi=0, \tag{5}$$

$$\chi=h=v=0 \quad \text{at} \quad \phi=\phi_e, \tag{6}$$

where ϕ_e is the edge angle. The numerical solution to equation (1) is obtained by splitting the shell into two regions separated by the ring load and enforcing the continuity conditions

$$\mathbf{y}^+=\mathbf{y}^-+[0, 0, P/2\pi, 0, 0, 0]^T \quad \text{at} \quad \phi=\phi_0 \tag{7}$$

where + and − denote the regions outside and inside the load, respectively. With the deflection $v^+ = v^- = \Delta$ specified at $\phi = \phi_0$, the corresponding load P is computed.

Each region is divided into N subintervals, and an initial solution is guessed. With a first-order polynomial employed to integrate the discretized shell equation (1), a Newton-Raphson method is used to converge on the correct solution. See Parnell (1984) or Cagan (1985) for more detail.

Care must be taken to include an adequate number of subintervals within the boundary layers near the load, the dimple edge, and the shell edge, where bending stresses change rapidly. Thus, the shell is actually divided into three regions (Fig. 2); regions I and II join at $\phi = \phi_0$, and, since the location of the dimple edge is not known *a priori*, regions II and III meet at some user-defined point $\phi = \alpha$ to allow for high accuracy within the decaying boundary layers. The decay angle is approximated as

$$\phi_{\text{dec}}=\pi\left(\frac{2c}{R}\right)^{1/2}, \tag{8}$$

where

$$c^2=\frac{t^2}{12(1-\nu^2)}. \tag{9}$$

Load-deflection curves were found by starting at zero load with $\mathbf{y} = \mathbf{0}$ and incrementing the deflection a small amount. After convergence, this solution became the initial guess at the next deflection, and so on. Based on the energy quantity

$$\|\mathbf{y}^{(k)}(s)\|_E=(|rM_\phi\cdot\chi|+|rH\cdot h|+|rV\cdot v|), \tag{10}$$

convergence at each point of the shell is obtained when the relative difference between the new and old solutions

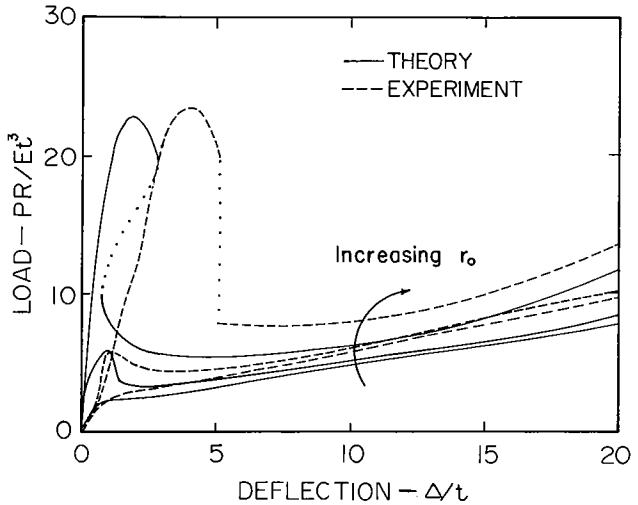

Fig. 3 Comparison of calculated load-deflection curves with experimental data of Evan-Iwanowski et al. (1963): R = 254 mm; R/t = 666.7; r_o = 6.35, 12.7, 25.4 mm

$$\epsilon = \frac{\|\mathbf{y}^{(k+1)}(s)\|_E - \|\mathbf{y}^{(k)}(s)\|_E}{\|\mathbf{y}^{(k+1)}(s)\|_E} \tag{11}$$

is less than a prescribed amount.

Shallow Shell

Evan-Iwanowski et al. (1963) presented experimental data for ring loads on die-pressed, plastic, shallow spherical shells. Figure 3 compares their experimental and our analytical results for a clamped shell of radius R = 254 mm.

As shown in Fig. 3, the load versus deflection curves for the smallest ring (r_0 = 6.35 mm) agree in general with no instabilities. Meanwhile, the experimental and theoretical results for the larger rings show similar trends, but the computed curves are steeper before the peaks. In addition, the calculated results peak at somewhat lower values of deflection than do the experimental results. This discrepancy is because the present model does not allow for slippage under the load; thus, the arc length of the shell inside the ring is assumed to remain constant. In reality there is not enough friction to maintain this constant contact and slippage does occur. Therefore, our model is slightly stiffer and buckles before the experimental shells.

While the second smallest ring (r_0 = 12.7 mm) demonstrates transition buckling, the largest ring (r_0 = 25.4 mm) illustrates local buckling with a discontinuity in the load. The analysis shows that these latter curves possess multiple equilibria over certain regions of deflection similar to the buckling of circular cylinders with axial load (Timoshenko and Gere, 1961). In order to obtain the section of the curve past the peak, the point-load solution at Δ/t = 8.2 was used as an initial guess for larger diameters at nearby deflections. Then the deflection was incremented (decremented) as before to obtain the remainder of the curve.

Figure 4 shows the changing shape of the shell for the largest ring load (r_0 = 25.4 mm). At Δ/t = 2.88, there is an abrupt change in shape. The dimple of reversed curvature forms suddenly during local buckling as the shell moves to a lower strain energy configuration. On the other hand, in transition buckling, the dimple forms gradually (see Fig. 1*a*).

Figure 5 shows the nondimensional bending stress ($\sigma R/2cE$; $\sigma = 6M_\phi/t^2$) versus meridional angle for the same shell and deflections. The bending stresses for the first two deflections (curves 1 and 2), which occur before buckling, peak under the load and then decay to zero in both directions. After the dimple forms during buckling, however, relatively constant bending stress develops inside the ring (curves 3 and 4). This

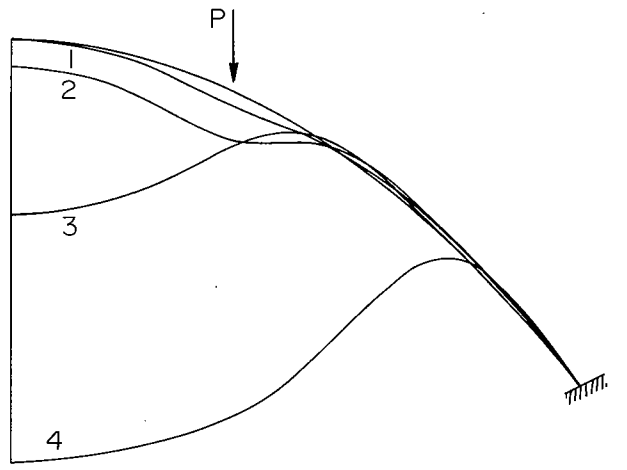

Fig. 4 Computed deformed configurations for shallow shell under ring load (r_0/R = 0.1; R/t = 666.7) for Δ/t = 0, 0.967, 2.88, 19.5. Local buckling occurs from configurations 2 to 3 at Δ/t = 2.88.

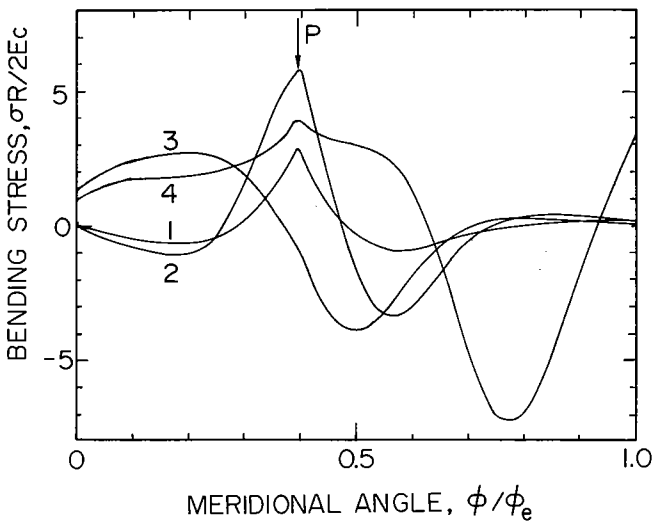

Fig. 5 Bending stress distribuitons along shallow shell with ring load (r_0/R = 0.1; R/t = 666.7). Curve numbers correspond to configurations of Fig. 4.

behavior agrees with the finding of Ashwell (1960), who studied the point-load solution to this problem and showed that a constant bending moment is necessary to hold the dimple in a state of reversed curvature, i.e., as an applicable surface.

The largest deflection (curve 4) shows peaks in stress under the load, at the dimple edge, and at the clamped shell edge. Just after buckling (curve 3) the trends are different; the peak at the dimple edge occurs, but the stress under the load is quite small. Here, the unstable shell transfers from a high energy state to a low energy condition, and so the load sees minimal restraint. The stress relaxes under the load until the shell stabilizes after buckling, and then additional load is applied.

Deep Shell

The behavior of deep shells under ring loads is similar to that of shallow shells. Taber (1983) presented experimental results for solid, cylindrical indenter loads on clamped, hemispherical rubber shells ($R \simeq 25$ mm). Although the present analysis is actually for pure ring loads, some conclusions can be made by comparing the results of the two problems. In Figs. 6(*a*)–6(*c*), new data is presented from those experiments,

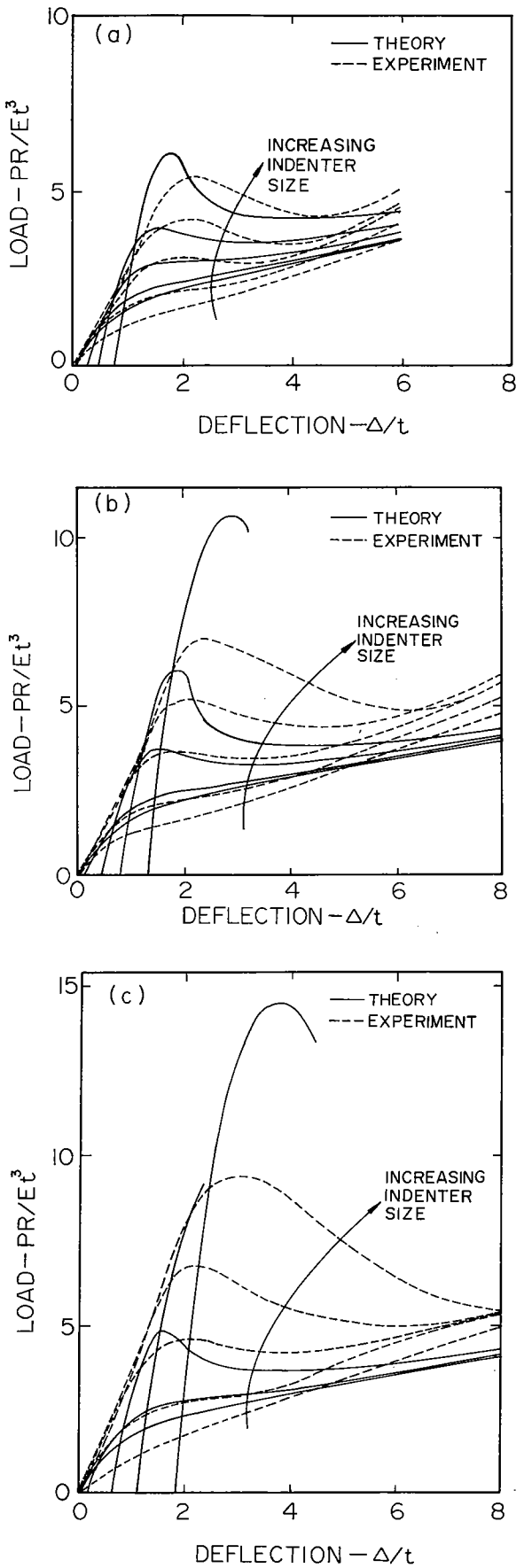

Fig. 6 Comparison of calculated load-deflection curves with experimental data from hemispherical shells with indenter loads: $R \simeq 25$ mm; $r_0 = 1.25, 3.75, 7.5, 10.0, 12.7$ mm; (a) $R/t = 6.0$; (b) $R/t = 9.6$; (c) $R/t = 12.9$

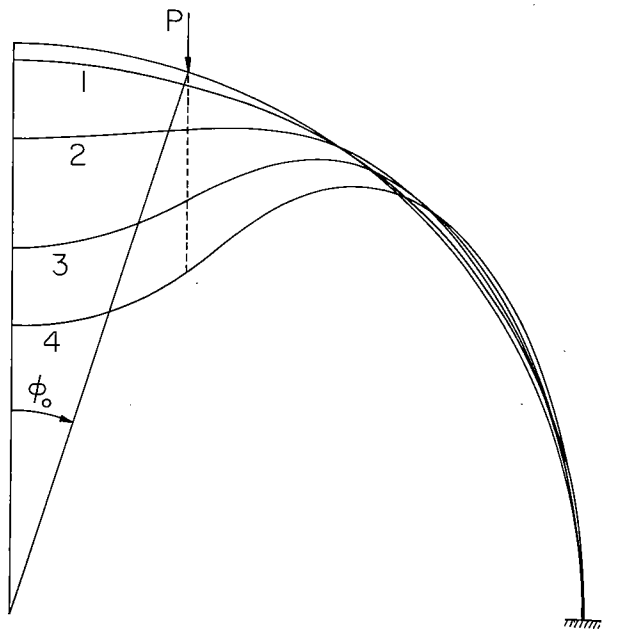

Fig. 7 Computed deformed configurations for hemispherical shell under ring load ($r_0/R = 0.3$; $R/t = 12.9$) for $\Delta/t = 0, 0.945, 2.27, 3.91, 5.55$

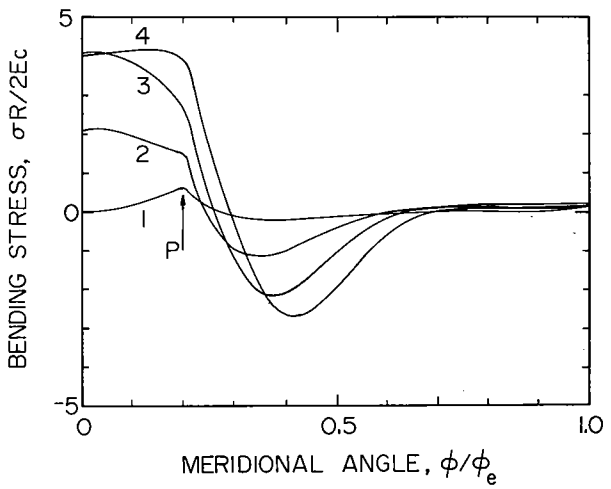

Fig. 8 Bending stress distribution along hemispherical shell with ring load ($r_0/R = 0.3$; $R/t = 12.9$). Curve numbers correspond to configurations of Fig. 7.

along with calculations from our model. Relatively thick to thin shells ($R/t = 6.0, 9.6, 12.9$) deformed by indenters of various radii are considered. As with the shallow shell, small indenters show no buckling. The discrepancy in load magnitude may be due to shear deformation, which was not included in the analysis. As the indenter size increases, transition buckling appears; the curves initially follow the relatively stiff behavior of a flat plate and then approach the limiting point load case.

Note that the computed solution does not begin at the origin. When the ring load forms, its point of zero deflection occurs at $\Delta = R\,(1 - \cos\phi_0)$ as measured from the apex, which was taken as the experimental reference point. Thus, the load initially is lower analytically than experimentally. But after the indenter makes full contact with the shell, forming a ring load, the solution approaches the experimental data.

Figure 7 shows the ring load representation for the indenter. Physically, a ring allows the shell inside the load ($\phi < \phi_0$) to penetrate above the point of load application. The solid indenter, however, obstructs this penetration and forces the entire area within the indenter radius to form a dimple from the

start. Thus, the experimental results show transition-buckling at smaller loads than do the analytic results, and local buckling does not occur under solid indenters.

The theoretical results from the thinner shells show local buckling for the larger indenters (Figs. 6*b*, *c*). For the thickest shell, however, this type of instability does not occur (Fig. 6*a*); due to the high bending stiffness, the ring forces the dimple to form from an early deflection, similar to the solid indenter case. The sharpness of the peaks during the transition buckling is also lost as the shell becomes thicker, approaching a three-dimensional solid, which does not buckle. As the deflection increases to large values, the theoretical and experimental curves diverge. The calculations are limited to moderate rotations and small strains, but at very large deflections, the physical shells undergo large rotations and large bending strains. In addition, the effects of material nonlinearity (Taber, 1985) may contribute to the difference.

Figure 7 demonstrates the calculated deflected shape of the thinnest shell ($R/t = 12.9$) with a 7.5 mm radius indenter. Since this indenter shows only transition buckling, these results illustrate a smooth formation of the dimple, unlike the abrupt change found in local buckling (Fig. 4).

Figure 8 displays the bending stress for the same shell and deflections. A negative peak forms at the dimple edge and then the stress decays toward zero before increasing slightly near the clamped edge ($\phi_e = \pi/2$). An abrupt change in slope occurs under the load. Again, as in Fig. 5, a relatively constant stress forms inside the dimple as the deflection increases.

Conclusions

The results of this study show that, for a given value of R/t for a spherical shell with a ring load of radius r_0, there exist characteristic ring load radii r_1 and r_2 with $r_1 < r_2 < R$ such that:

(1) For $r_0 < r_1$, no buckling occurs and the solution resembles that for a point load.
(2) For $r_1 < r_0 < r_2$, transition buckling takes place in which the load rises to a peak and then drops off toward the point-load curve.
(3) For $r_2 < r_0 < R$, the shell buckles locally, with an abrupt change in shape and load at a critical deflection.

In addition, the values of r_1 and r_2 increase as the shell thickness increases. These conclusions apply to both shallow and deep shells with clamped edges. For a solid, cylindrical indenter, the behavior is similar, but local buckling does not occur.

References

Ashwell, D. G., 1960, "On the Large Deflection of a Spherical Shell with an Inward Point Load," *Proceedings of the IUTAM Symposium on the Theory of Thin Elastic Shells*, Koiter, W. T., ed., North Holland, Amsterdam, pp. 43–63.

Cagan, J., 1985, "Large Deflection of a Deep Spherical Shell Due to Rigid Indenters of Various Radii," Master's Thesis, University of Rochester.

Chien, W. Z., and Hu, H. C., 1956, "On the Snapping of a Thin Spherical Cap," *Proceedings of the 9th International Congress of Applied Mechanics*, Brussels, Belgium, pp. 309–320.

Evan-Iwanowski, R. M., Loo, T. C., and Tierney, D. W., 1963, "Local Buckling of Shells," *Developments in Mechanics*, Vol. 2, Ostrach, S., and Scanlan, R. H., eds., Pergamon, New York, pp. 221–251.

Parnell, T. K., 1984, "Numerical Improvement of Asymptotic Solutions and Nonlinear Shell Analysis," Ph.D. Thesis, Stanford University.

Reissner, E., 1950, "On Axisymmetrical Deformations of Thin Shells of Revolution," *Proceedings of the Third Symposium in Applied Mathematics*, McGraw-Hill, New York, pp. 27–52.

Taber, L. A., 1983, "Compression of Fluid-Filled Spherical Shells by Rigid Indenters," ASME JOURNAL OF APPLIED MECHANICS, Vol. 50, pp. 717–722.

Taber, L. A., 1985, "On Approximate Large Strain Relations for a Shell of Revolution," *International Journal of Nonlinear Mechanics*, Vol. 20, pp. 27–39.

Timoshenko, S. P., and Gere, J. M., 1961, *Theory of Elastic Stability*, McGraw-Hill, New York.

Updike, D. P., and Kalnins, A., 1970, "Axisymmetric Behavior of an Elastic Spherical Shell Compressed Between Rigid Plates," ASME JOURNAL OF APPLIED MECHANICS, Vol. 37, pp. 635–640.

Updike, D. P., and Kalnins, A., 1972, "Axisymmetric Postbuckling and Nonsymmetric Buckling of a Spherical Shell Compressed Between Rigid Plates," ASME JOURNAL OF APPLIED MECHANICS, Vol. 39, pp. 172–178.

Wan, F. Y. M., 1984, "Shallow Caps with a Localized Pressure Distribution Centered at the Apex," *Flexible Shells, Theory and Applications*, Axelrad, E. L., and Emmerling, F. A., eds., Springer-Verlag, New York, pp. 124–145.